16

Uncertainty Quantification and Propagation for Projections of Extremes in Monthly Area Burned Under Climate Change: A Case Study in the Coastal Plain of Georgia, USA

Adam J. Terando,[1] Brian Reich,[2] Krishna Pacifici,[3] Jennifer Costanza,[4] Alexa McKerrow,[5] and Jaime A. Collazo[6]

ABSTRACT

Human-caused climate change is predicted to affect the frequency of hazard-linked extremes. Unusually large wildfires, individually or expressed as area burned over time, are a type of extreme event that is constrained by climate and can be a hazard to society but also an important ecological disturbance. Here we project changes in the frequency of extreme monthly area burned by wildfires for the end of the 21st century for a wildfire-prone region in the southeast United States. Predicting changes in area burned is complicated by the large and varied uncertainties in how the climate will change and in the models used to predict those changes. We characterize and quantify multiple sources of uncertainty and propagate the expanded prediction intervals of future area burned. We find nontrivial probabilities for an increasing number of extreme wildfire months for the period 2070–2099 (95% projection interval of 5 fewer to 28 more extreme fire months for a high fossil-fuel emissions scenario), resulting from the warmer climate, but also due to the inherent uncertainty when dealing with extreme events. Our approach illustrates that while accounting for multiple sources of uncertainty in global change science problems is a difficult task, it will be necessary in order to properly assess the risk of increased exposure to these society-relevant events.

[1] *US Geological Survey, Southeast Climate Science Center, Raleigh, North Carolina, and Department of Applied Ecology, North Carolina State University, Raleigh, North Carolina, USA*

[2] *Department of Statistics, North Carolina State University, Raleigh, North Carolina, USA*

[3] *Department of Forestry and Environmental Resources, Program in Fisheries, Wildlife, and Conservation Biology, North Carolina State University, Raleigh, North Carolina, USA*

[4] *Department of Forestry and Environmental Resources, North Carolina State University, Raleigh, North Carolina, USA*

[5] *Department of Applied Ecology, North Carolina State University, Raleigh, North Carolina, and Core Science Analytics, Synthesis & Libraries, US Geological Survey, Raleigh, North Carolina, USA*

[6] *Department of Applied Ecology, North Carolina State University, Raleigh, North Carolina, and US Geological Survey, North Carolina Cooperative Fish and Wildlife Research Unit, North Carolina State University, Raleigh, North Carolina, USA*

16.1. INTRODUCTION

Human-caused global warming (that is, *anthropogenic* climate change, or ACC) has the potential to increase exposure to hazards by increasing the frequency or severity of damaging extreme events [*Walsh et al*., 2014]. Extreme wildfires present one of the most visible and concerning examples of a hazard that could be affected by ACC because of the potential for large-scale destruction and disruption of human-dominated landscapes. And yet, although wildfires can be a hazard, they are also a vital part of ecosystem disturbance and nutrient cycling dynamics [*Certini*, 2005]. As such, efforts to promote ecologically beneficial fires, which can also reduce the risk of damaging fires and promote system resilience, will suffer if changing climatic conditions increase the risk of

Natural Hazard Uncertainty Assessment: Modeling and Decision Support, Geophysical Monograph 223, First Edition.
Edited by Karin Riley, Peter Webley, and Matthew Thompson.

large uncontrollable fires [*Ryan et al.*, 2013]. Furthermore, in areas with large unfragmented forest ecosystems, increases in wildfire activity or the area burned by wildfires could also impact the global carbon cycle, further exacerbating ACC through the rapid release of carbon from forests [*Liu et al.*, 2014].

Recent studies have shown that some regions are currently experiencing more frequent large wildfires due to more conducive climatic conditions linked to ACC [*Dennison et al.*, 2014]. Given the changes already observed, and the strong expectation that global warming will accelerate in the future, researchers have developed models to predict how future ACC could impact different aspects of wildfire regimes, such as the frequency of large wildfires [*Girardin and Mudelsee*, 2008], the severity of wildfires as characterized by burn rates [*Fried et al.*, 2004], and the total area burned [*Litschert et al.*, 2012]. The potential for future changes in extreme wildfire occurrence or as expressed as the total area burned is an example of an indirect consequence of ACC. Unlike direct consequences of ACC or changes to the climate system itself (e.g., changes in climate phenomena such as temperature, precipitation, and hurricanes) that can be modeled solely through the use of climate models, indirect consequences require additional models to link the climate forcing to the ecological response. And with this additional layer of modeling comes additional uncertainty associated with the predicted consequences of ACC because of our imperfect knowledge of the system and the future.

Uncertainties in the context of global change have been extensively explored and debated within the climate science literature, particularly with regard to how best to characterize and quantify uncertainty given our inability to (1) construct controlled experiments on the climate system, (2) make deterministic predictions for this highly nonlinear system beyond 2–3 weeks [*Lorenz*, 1963], or (3) resolve many key processes in the climate system [*Palmer et al.*, 2005]. Generally, in climate change prediction problems (and likely the broader class of global change prediction problems), three forms of uncertainty are identified: internal variability, scenario uncertainty, and structural uncertainty [*Hawkins and Sutton*, 2009]. Internal or "natural" variability refers to the unforced variability that arises in highly nonlinear complex systems such as the Earth's climate system. Scenario uncertainty in the context of ACC refers to uncertainty in future anthropogenic emissions of greenhouse gases that lead to a perturbed climate response. While multiple models may be used to evaluate the same or alternate scenarios, by definition no formal likelihood or probability structure is attached to each independent vision of the future. Finally, structural uncertainty, or model uncertainty, occurs when competing models exist to describe the unknown state of nature relative to the parameter of interest, represented as θ [*Draper*, 1995]. Each general circulation model (GCM) that is a member of a larger ensemble of models (such as those found in the Coupled Model Intercomparison Project[s]) represents a particular set of assumptions about how nature (i.e., the climate system) operates which can be used to make predictions about θ. We also note that a fourth type of uncertainty, parametric uncertainty, is also present and represents uncertainty about parameters within or common to the individual models that affect the predictive uncertainty about θ [cf. *Sriver et al.*, 2012]. Depending on the problem and context, this form of uncertainty is sometimes subsumed under the more general category of structural or model uncertainty.

With these forms of uncertainty defined, the question becomes how to characterize and quantify each so that predictions are most useful to decision makers. Typically, usefulness in this context is defined as providing predictions about the future state of θ that maximize sharpness in a probabilistic sense (subject to calibration) [*Gneiting et al.*, 2007] while also avoiding underdispersion, which leads to overconfident predictions [*Draper*, 1995; *Raftery et al.*, 2005]. Note that this formulation focuses on probabilistic predictions, suggesting that a Bayesian approach (or at least partially Bayesian when considering calibration [*Draper*, 2013]) is appropriate to quantify uncertainty.

Various methods have been employed to account for these sources of uncertainty, particularly as it relates to structural uncertainty in climate models. Sometimes referred to as "kernel dressing," these methods transform point predictions into distributional functions that allow for a formalization of the degree of belief that is assigned to each model's prediction [*Brocker and Smith*, 2008]. Bayesian Model Averaging (BMA) [*Raftery et al.*, 1997], an increasingly popular way to quantify uncertainty across competing models, has been employed in fields such as meteorology [*Raftery et al.*, 2005], climate change science [*Terando et al.*, 2012], and ecology [*Wintle et al.*, 2003] where forecasts or predictions normally must be developed for nonlinear, unbounded systems characterized by partial observability, partial controllability, or both. However, far fewer attempts have been made to *combine* and *propagate* the independent forms of uncertainty in global change predictions where models of climatic responses to fossil fuel emissions are linked to indirect ACC consequences such as changes in large wildfires. Fully propagating uncertainty from ACC scenarios to climate models to ecological models is certainly a nontrivial task. But if predictions are to be of use to decision makers that must adapt or respond to ACC impacts on ecosystems, then attempts to more fully characterize and quantify both climate model and ecological model uncertainty will be necessary.

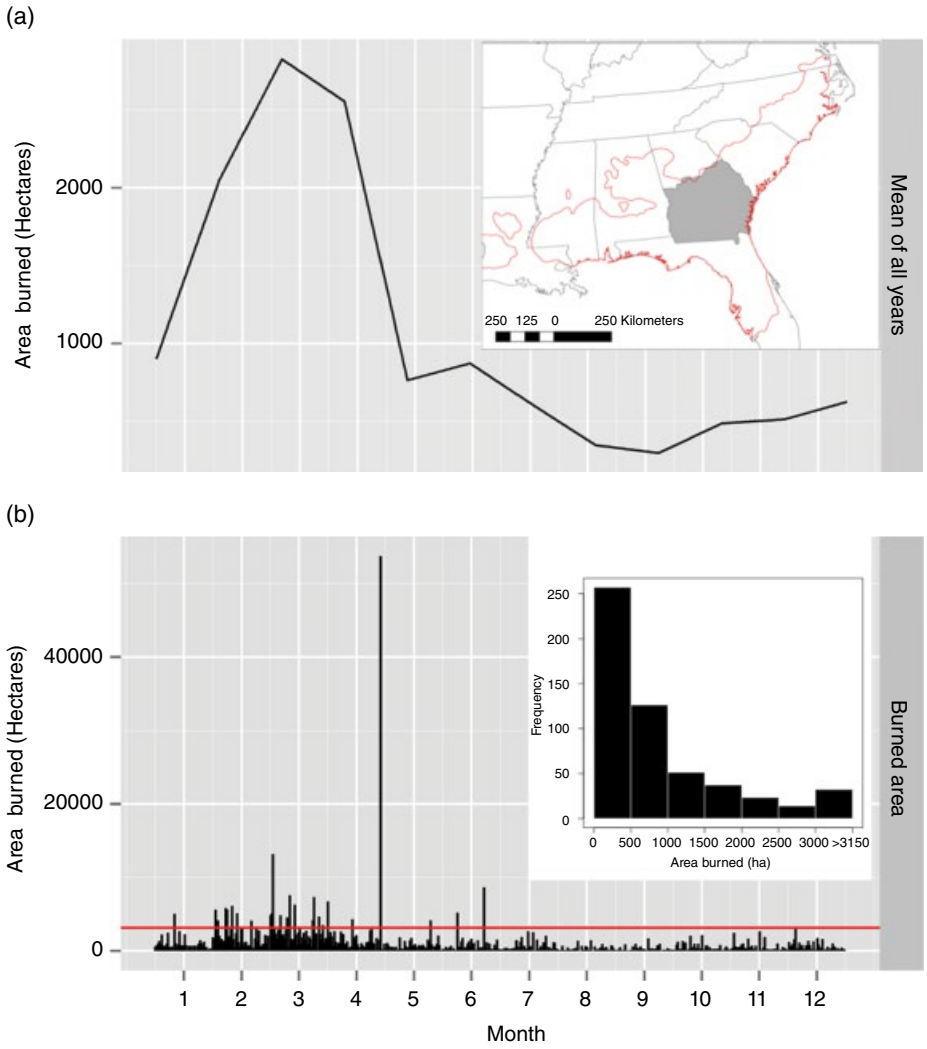

Figure 16.1 Wildfire characteristics in the study region: (a) Mean monthly area burned over the period 1966–2010; (b) monthly area burned over the period of record (1966–2010) and the 96th sample quantile (horizontal red line, equal to 4047 ha or ~10,000 acres). Also shown is the study area in the context of the historic range of the longleaf pine (inset in [a]) and the histogram of observations in the inset in (b).

Here we provide an example of fully propagated structural uncertainty in a global change prediction problem, in which θ represents *months with an unusually large (i.e., extreme) amount of hectares burned by wildfires* (hereafter denoted as EBA for extreme burned area) across the coastal plain region of Georgia, USA (Fig. 16.1). The model is developed in the context of the longleaf pine ecosystem, a critically endangered and highly altered pyrophytic ecosystem in the southeastern United States. In this system, the response of θ to ACC is highly uncertain but requires that decision makers develop conservation plans that account for a changing climate. We use BMA to quantify structural uncertainty among competing ecological models that relate climatic conditions to EBA months, as well as among the actual climate models. Internal climate variability is estimated and incorporated into the BMA when deriving model-specific weights. Scenario uncertainty is assessed by examining the results in light of multiple fossil fuel emissions trajectories. Our work provides a template for global change studies that must account for and propagate uncertainty about the effects of ACC in a way that informs natural resource decision makers.

16.2. DATA

16.2.1. Study Area

We focus on a 9 million ha region of the coastal plain of Georgia, USA (Fig. 16.1). The mix of land uses, the occurrence of large natural areas, as well as the recent

occurrence of several extreme fires make the region an ideal study area for our research. The region is dominated by agricultural and forest land uses, with rural communities distributed throughout. Several public landholdings with large natural areas are present, including the US Fish and Wildlife Service's Okefenokee National Wildlife Refuge. Historically, wildfires across the southeast coastal plain were very common and although individual fires could cover vast tracts of land (>1000 km^2), burn intensities were low and crown fires rare [*Frost*, 2006; *Peet*, 2006]. For example, savannas dominated by longleaf pine (*Pinus palustris*) once covered millions of hectares in the southeast United States and burned as frequently as every 1–3 yr [*Brown and Smith*, 2000]. When frequently burned, this ecosystem can harbor among the highest levels of plant diversity in the world [*Peet and Allard*, 1993]. However, because of recent fire suppression and forest conversion, the ecosystem is now critically endangered [*Noss et al*., 1995]. This fire suppression occurs directly through firefighting activities, but also indirectly through fragmentation of the landscape, which increases fire breaks and decreases the ability of any single ignition to spread across the landscape [*Frost*, 1993]. This active and passive fire suppression has resulted in much less frequent fire return intervals compared to pre-European settlement conditions. *Costanza et al*. [2015], for example, examined wildfire records for the coastal plain regions of Alabama, Georgia, and Florida and found wildfire return intervals that ranged from ~40 yr for surface fires in early succession longleaf pine forests to over 100 yr in degraded sites. Although wildfire return intervals are now much longer resulting in less area burned across the landscape, the peak fire season still occurs in the spring (Fig. 16.1) when large amounts of fine dead fuels (such as grasses and pine needles) from the previous winter are present and when humidity levels are low.

Even though wildfires are a natural part of all ecosystems in the coastal plain, large, high-intensity fires still pose unique risks to ecosystems, human health, and property, and are costly to manage. For example, within the past decade in this study area, the Okefenokee Refuge has experienced two extreme fire events. The Big Turnaround Complex Fire in 2007 was the most costly fire ever in the US Fish and Wildlife Refuge System [*US Fish and Wildlife Service*, 2007], burning over 388,000 acres. Only 4 yr later, the Honey Prairie Fire started in the swamp and burned for over 11 mo, involving over 1400 personnel [*US Fish and Wildlife Service*, 2012]. These wildfires impacted ecological communities [*Beganyi and Batzer*, 2011] and emitted aerosols that can affect human health [*Bhoi et al*., 2009]. Some fires on the southeast coastal plain can also be intense ground fires that consume large amounts of fuel contained in peat soils [*Poulter et al*., 2006]. These fires can lead to high carbon emissions, while also retarding peat development and vegetation recovery following the fire [*Poulter et al*., 2006; *Richardson*, 2012]. Given the impacts of extreme events such as these, the difficulty of managing them, and the potential for climate change to alter wildfire regimes, it is important to quantify the uncertainty associated with wildfires in this region in order to better plan and manage the risks they pose.

16.2.2. Wildfire Observations

Monthly wildfire records were obtained for the period 1966–2010 for counties in the study area (Fig. 16.1d; *Chan*, Georgia Forestry Commission, unpublished data). We aggregated the monthly area burned across all counties into a single value for the entire study area for each month from 1966 to 2010. The wildfire data are based on state agency records of reported wildfires. Thus, some biases may exist in the data; for example, small fires may have been underreported. However, large fires are likely captured in these data, making them well suited for our purpose of modeling extremes. Furthermore, while other studies have reported bias in wildfire records over time due to changes in reporting methods through time [*Littell et al*., 2009], because the data for Georgia were collected and distributed by a single agency, this bias should be reduced. A bias is apparent for the years prior to 1966, wherein the time series of monthly burned area is less variable (i.e., a "smoother" time series). This likely marks the point at which reporting methods changed, leading to more accurate and precise surveys of wildfire size. The combination of better reporting of wildfires, continual data collection by a single agency, and a stationary (log-transformed) time series from 1966 to 2010, indicates that this dataset is appropriate to use to evaluate the relationship between climate and EBA months.

16.2.3. Climate Data and Models

Climate data are taken from [*Maurer et al*., 2002], a 12 km resolution gridded dataset of daily meteorological observations from 1950 to 2010. After calculating derived daily climate variables such as diurnal temperature range (see Section 16.3.1), we average the daily values over space and time to obtain monthly time series of these variables for the study region for the same period as the wildfire observations (1966–2010). We use bias-corrected statistically downscaled climate model output for our ensemble of climate projections [*Stoner et al*., 2013]. The downscaled models are derived from GCM output produced as part of the Third Coupled Model Intercomparison Project [CMIP3; *Meehl et al*., 2007]. The downscaled models are bias corrected to the [*Maurer*

et al., 2002] dataset, have the same spatial and temporal resolution, and have output available for the period 1960–2099. The composition of the GCM ensemble varies by emission scenario, with 8, 6, and 11 models available for the B1, A1b, and A2 scenarios, respectively (see Table 16.3 in Section 16.4.2).

16.3. METHODS

16.3.1. Structural Uncertainty in the Ecological Model

We build a statistical model to predict extremely large values of the number of hectares burned per month (EBA) Y_t as a function of covariates, X_t Our use of monthly burned area as our measure of interest is based on issues of practicality and utility. First, while the ignition and spread of individual fire events will respond strongly to short-term fluctuations in variables such as wind speed and relative humidity (affecting fuel moisture) or lightning (affecting ignition probability), average monthly climate variables will still reflect the broad-scale climatic conditions that are necessary for extreme wildfires to occur. Second, few long-term wildfire databases exist for the Southeast that encompass a large sample of EBA months. Using the monthly wildfire database available from the Georgia Forestry Commission (see Section 16.2.2) with a period of record that stretches back to the 1960s allows for a more robust estimation of the parameters used to predict extremes. Finally, we argue that projecting changes to EBA months is consistent with the scale or specificity of planning conducted by managers with regard to climatic changes occurring over multiple decades in the future.

The covariates X_t include an intercept (I), the mean monthly diurnal temperature range (T_{dn}), the mean monthly maximum daily temperature (T_{mx}), the detrended with seasonal cycle removed maximum daily temperature (T_{anom}), and the 3 mo (short-term) and 24 mo (long-term) standardized precipitation index (SPI) values (SPI_3, SPI_{24}) [*Guttman*, 1998]. Diurnal temperature range is used to represent atmospheric moisture content, an important consideration for fuel moisture content. More direct measures of moisture content such as relative humidity were ultimately not able to be included because of the limited set of climate variables available in the statistically downscaled climate model dataset. We do not consider ignition source in this model since our interest lies in predicting the occurrence of EBA months. Regardless of whether the ignition was due to lightning or humans, the occurrence of an EBA month reflects an inability to rapidly extinguish wildfires due to fuel and climatic conditions.

Three seasonal terms (S_1, S_2, S_3) are included based on the amount of chilling hours [*Fishman et al*., 1987], which we use to signal the onset and termination of the growing season, and therefore the changing ratio between dry combustible fuels and wet noncombustible fuels. This also allows for dynamic seasons whose length can change as the climate warms. Season S_1 corresponds to the high fire season in the late winter and early spring, S_2 coincides with the nadir of the fire season in the summer months when moisture levels are high and available combustible fuels are low, and S_3 is the fall and winter season when more acreage is typically burned than in the S_2 season but extremes in monthly area burned are rare (Fig. 16.1). For simplicity, we refer to the seasons S_1, S_2, S_3 as the spring, summer, and fall fire seasons. We also include interactions between each of these 6 covariates and the three season indictors giving a total of 18 covariates in X_t, to account for differences in fire patterns by season.

To estimate the relationship between climate and EBA months, the model is initially fit with X_t taken to be the observed monthly weather values from the *Maurer et al*. [2002] dataset for the years 1966–2010. Because of the large number of covariates and the small number of EBA months, we consider several statistical models defined by subsets of the 18 variables. We averaged over predictions from the statistical models using Bayesian Model Averaging (BMA). BMA [*Raftery et al*., 1997] allows for a probabilistic estimation of structural uncertainty between models by producing a weighted predictive distribution according to relative skill of each candidate model (cf. *Wintle et al*. [2003] for a discussion of BMA in ecological applications). The BMA predictive model for observation Y_t is:

$$f\left(Y_t \mid Y_0\right) = \sum_{k=1}^{k} f\left(Y_t \mid M_k\right) Prob\left(M_k \mid Y_0\right), \quad (16.1)$$

where $M_1, \ldots, M_k$ are the k competing models, and Y_o is the training data used to fit the model.

We use a points-above-threshold analysis [*Cole*, 2001] for extreme events (EBA months). Observations are considered extreme if they exceed the threshold T hectares. We use fivefold cross-validation to select a value of T that maximizes model skill based on comparison of Brier scores [*Brier*, 1950] and quantile scores. The covariates are included in both the probability of exceeding the threshold and the severity of exceedances. We use logistic regression to model exceedance probabilities

$$logit\left[Prob\left(Y_t > T\right)\right] = X_t^T \beta_1 \quad (16.2)$$

Exceedances of the threshold T are modeled using the generalized Pareto distribution (GPD). The GPD has two parameters: scale $\sigma_t > 0$ and shape ξ. Under the GPD

model, the conditional probability of exceeding y hectares burned is

$$Prob\left(Y_t > y \middle| Y_t > T\right) = \left[1 + \frac{\xi}{\sigma_t}\left(y - T\right)\right]^{-\frac{1}{\xi}} \quad (16.3)$$

The shape parameter controls the tail behavior, with large and positive ξ corresponding to a heavy tail and thus very large extreme values and negative ξ corresponding to a bounded distribution without severe extremes. In our analysis, we allow the scale parameter to vary with covariates, $\log(\sigma_t) = X_t^T \beta_2$. The shape parameter is held constant over time because this parameter is notoriously difficult to estimate. We assume all subsets of covariates are equally likely a priori and that the same subset of covariates appears in the logistic probability of an EBA month and the GPD log scale parameter. The covariates are centered and scaled to have mean zero and variance one, and the elements of β_j have prior normal distributions of $N(0, \sigma^2)$, where the variances σ^2 have inverse-gamma priors of (0.1,0.1). Finally, the GPD shape parameter has a $N(0, 0.25^2)$ prior. We note that regardless of the *decision-dependent* definition of a catastrophic fire (tied to actual economic and environmental losses), we assume that our model-based selection of T will be sufficiently low to permit inference on the actual decision-relevant threshold.

16.3.2. Structural and Emissions Uncertainty in the Climate Models

The ensembles of downscaled climate models contain structural uncertainty due to different parameterizations and model resolutions, leading to different predictions given the same climate forcings. We again use BMA to account for this structural uncertainty. *Terando et al.*, [2012], used a bootstrapping procedure to gauge climate model prediction skill for long-term evolving temperature trends. In brief, training datasets of the estimated trend over a 50 yr period (1961–2010) are constructed for the observations and downscaled GCM output. The temporal trends form the basis of the estimated model skill that is used to estimate the BMA weights. The bootstrapping procedure is used to estimate the uncertainty around the trend by sampling 1000 times from the residuals of a best fit statistical model of the trend in the observations and climate model output. Both linear and polynomial models are fit based on AIC selection and after accounting for autocorrelation in the residuals. These resampled residuals are then recombined with the trend estimate and a new trend estimate is produced. The result is 1000 pseudo time series for each observed and modeled climate variable that reflects decadal climate variability and the ability of the downscaled GCMs to reproduce the observed time-evolving trends. This method limits spuriously low or high model weights that can result from using BMA with climate models whose experiments use observed climate forcings, but are not meant to simulate the actual observed weather. It also implicitly takes into account the internal unforced variability of the climate system (see *Terando et al*. [2012] for further details). We extend the univariate model in that work to the multivariate case and evaluate model skill for the downscaled ensemble for maximum temperature, diurnal temperature, 3 mo SPI, 24 mo SPI, and monthly precipitation.

Scenario uncertainty is evaluated in the standard manner by comparing results for multiple fossil fuel emission scenarios. We compare three emission scenarios used in the Fourth Assessment Report of the Intergovernmental Panel on Climate Change (AR4 IPCC) corresponding to a low (B1), medium (A1b), and high (A2) future level of fossil fuel emissions [*Nakicenovic et al*., 2000]. Based on our structural uncertainty characterization in the joint ecological-climatological model, we substitute the BMA posterior distribution for X_t to make predictions for two 30 yr periods, present (1980–2009) and future (2070–2099), conditional on the chosen emission scenario, to evaluate the potential for ACC to increase the number of EBA months in this region.

16.4. RESULTS

16.4.1. Cross-Validation Results and GPD Fitted Parameters

The Brier scores and quantile scores from the fivefold cross-validation indicated that a threshold T of 1465 ha burned provides the best estimate of the GPD parameters for predicting EBA months with 4047 or more hectares burned. This threshold corresponds to the 0.8 sample quantile over the 45 yr observation period. Brier scores were similar for the three quantiles (0.5, 0.8, 0.95) that were tested against six extreme quantiles for prediction (Table 16.1). However the quantile scores were lowest (lower error) for the 0.8 quantile across all EBA thresholds above the prediction 0.8 quantile. Given the larger relative differences between the quantile scores that favored using the 0.8 quantile threshold compared to the Brier scores, we used the 0.8 quantile to fit the GPD parameters. This threshold likely represents a compromise between lower thresholds that increase the number of observations available for fitting the model and higher thresholds that are more representative of the processes that are responsible for EBA months.

The 90% posterior interval for the GPD shape parameter ξ is [0.11, 0.44]. The shape is positive so the

distribution of extreme monthly burned area is unbounded; however, the shape parameter is less than 0.5 so the distribution is not extremely heavy-tailed and has finite mean and variance. The posterior probabilities that each covariate in X_t is included in the statistical model of EBA months range from a low of 0.08 (T_{anom}.S_1) to 1 for the three seasonal intercept terms and diurnal temperature in the high fire season (Table 16.2). Consistent with the peak fire season occurring when conditions are dry and combustible fuels are present, there is strong support for inclusion of the spring season diurnal temperature (positive posterior mean values) and three month SPI covariates (negative posterior mean values). Note that the estimated posterior means

Table 16.1 Brier Scores and Quantile Scores for the Ecological Model Based on Fivefold Cross Validation for Three EBA Thresholds Tested Against Six Prediction Thresholds

		Threshold Tested					
Score Criteria	*T*	0.95	0.96	0.97	0.98	0.99	0.995
Brier	0.5	0.040	0.033	0.028	0.018	0.011	0.006
	0.8	0.041	0.034	0.029	0.019	0.011	0.006
	0.95	0.043	0.035	0.029	0.019	0.012	0.006
Quantile	0.5	2215	2036	1807	1484	1015	730
	0.8	1536	1382	1210	1025	809	643
	0.95	2891	2551	2175	1748	1235	911

Note: Lower scores in both cases indicate less error between the model prediction and the verifying observations.

Table 16.2 Estimated Bayesian Model Averaging Probabilities $\left([\mathrm{P}(\beta)]_j \neq 0\right)$ for the Climate and Seasonal Covariates (X_t) and Best-Fit Values for the β_j Used to Estimate the Probability of Exceeding a Threshold (Hectares Burned Month^{-1}), β_1, and the Magnitude of the Extreme Burned Area, β_2.

		β_1			β_2		
X_t	$P(\beta_j \neq 0)$	μ	σ	90% CI	μ	σ	90% CI
$I.S_1$	1	−0.78	0.31	[−1.31,−0.32]	7.51	0.30	[6.99,7.97]
$T_{dn}.S_1$	1	1.00	0.28	[0.56,1.48]	0.50	0.21	[0.16,0.84]
$T_{mx}.S_1$	0.29	−0.10	0.24	[−0.65,0]	−0.09	0.21	[−0.57,0]
$T_{anom}.S_1$	0.08	0.00	0.05	[0,0]	0.00	0.04	[0,0]
$SPI_3.S_1$	0.69	−0.28	0.26	[−0.72,0]	−0.25	0.21	[−0.59,0]
$SPI_{24}.S_1$	0.1	0.02	0.08	[0,0.19]	0.01	0.05	[0,0.06]
$I.S_2$	1	−3.02	0.74	[−4.37,−2.09]	7.06	0.59	[5.99,7.89]
$T_{dn}.S_2$	0.98	0.98	0.40	[0.33,1.64]	0.36	0.31	[−0.1,0.9]
$T_{mx}.S_2$	0.67	0.68	0.76	[0,2.08]	0.24	0.50	[−0.39,1.2]
$T_{anom}.S_2$	0.38	0.11	0.28	[−0.14,0.73]	0.18	0.32	[0,0.89]
$SPI_3.S_2$	0.46	0.18	0.28	[0,0.78]	0.13	0.25	[−0.1,0.67]
$SPI_{24}.S_2$	0.26	−0.03	0.14	[-0.34,0.08]	0.05	0.17	[−0.03,0.44]
$I.S_3$	1	−2.52	0.62	[−3.65,−1.72]	7.28	0.56	[6.24,8.07]
$T_{dn}.S_3$	0.27	0.10	0.25	[0,0.71]	−0.01	0.21	[−0.42,0.32]
$T_{mx}.S_3$	0.57	−0.39	0.48	[−1.31,0]	−0.14	0.42	[−0.94,0.44]
$T_{anom}.S_3$	0.28	−0.04	0.17	[−0.42,0.1]	−0.08	0.19	[−0.53,0]
$SPI_3.S_3$	0.66	−0.33	0.34	[−0.93,0]	−0.35	0.37	[−1,0]
$SPI_{24}.S_3$	0.27	0.05	0.16	[−0.04,0.41]	−0.09	0.22	[−0.58,0]

Note: The covariates are included in the model estimation of both the probability of exceeding the EBA threshold and the severity of EBA.

for the spring season T_{dn} are the largest in absolute terms amongst all nonintercept covariates. It is interesting that T_{mx} and SPI_3 have the largest probabilities in the fall season, but T_{mx} has negative posterior means, suggesting that while "warm and dry" conditions increase the probability of EBA months in the spring season, "cool and dry" conditions are more important in the fall (but with fewer and less extreme EBA months overall).

16.4.2. GCM BMA Weights

The posterior climate model weights for the full ensemble in the A2 scenario include many low model probabilities (Table 16.3). The median model weight is 0.06, compared with the prior probability of 0.09 for an equally weighted model ensemble (where $n = 11$). Only two models have posterior probabilities of 0.18 or higher (twice the prior probability). Model weights are rebalanced for the other two emission scenarios since fewer GCMs are available, resulting in model weights as high as 0.39 in the case of the A1b scenario.

16.4.3. Projected Extreme Fires

Figure 16.2 shows the histogram of simulations and PDFs of the posterior predictive distributions for the number of months with 4047 ha (10,000 acres) or more burned over a 30 yr period (corresponding to the 0.96 quantile for the observation period). In Figure 16.2a, the histogram of 10,000 simulation results from the cross-validated predictive distribution for the 30 yr period that overlaps with the observations, indicates good agreement between the ecological model and the actual observed number of extreme burn months (vertical dashed line, equal to 12 EBA months). Similarly, the BMA-based joint ecological-climatological model PDF shows that the verifying observation is near the fiftieth percentile of the downscaled ensemble over the same 30 yr period (Fig. 16.2b).

Table 16.3 BMA Model Weights for Each Emissions Scenario for the Empirically Downscaled Members of the CMIP3 GCM Ensemble Based on Observations and Simulations From the 20C3M Experiment

		Model Weights		
n	Model	A2	B1	A1b
1	ccsm3.0	0.17	0.19	
2	cgcm3.1(T47)	0.02	0.03	0.03
3	cgcm3.1(T63)	0.12	0.13	0.19
4	cnrm	0.01	0.01	0.02
5	echam5	0.18	0.20	0.28
6	echo	0.25	0.28	0.39
7	gfdl-cm2.0	0.04	0.04	
8	gfdl-cm2.1	0.11	0.12	
9	hadcm3	0.01		
10	hadgem	0.06		0.09
11	pcm	0.04		

Note: Blank spaces indicate the absence of GCM output for that particular emissions scenario.

For the forward simulations depicting the projected probability of EBA months at the end of the 21st century (2070–2099), "long tails" in the BMA PDFs (solid black lines) are present for all three emissions scenarios, indicating an increased probability for more frequent EBA months (Fig. 16.2c–e). The 95% projection intervals for the B1 (low emissions level), A1b (medium emissions level), and A2 (high emissions level) scenarios are [−5, 18], [−4, 33], and [−6, 28], respectively. The 50th percentile value for the B1 scenario shows 0.7 more EBA months in the future, 0.2 more EBA months for the A1b scenario, and 0.5 fewer months for the A2 scenario. Accordingly, all scenarios indicate that roughly half of the PDF area lies above zero and that the long heavy tails are skewed toward an increase in extreme wildfire months. The apparently nonlinear relationship between the upper bounds of the projection interval and the emission scenario (i.e., a longer tail in the A1b scenario compared to the A2 scenario) is due to the reduced number of GCMs available for the A1b scenario, which causes a higher weight to be placed on one or more models that project more frequent EBA months. When the same set of models is used for the B1, A1b, and A2 emissions scenarios, the 95% intervals are [−5, 21], [−4, 31], and [−5, 30], respectively, resulting in very similar results for the mid- and high-emissions scenarios while still showing smaller increases in EBA months for the low-emissions scenario.

16.5. DISCUSSION

The potential for increases in EBA months is likely due to longer and hotter summer wildfire seasons that increase the probability for large fires relative to historic conditions. Most GCM projections of the diurnal temperature range remain constant or show declines over time, indicating that this variable is not contributing to the projected increases, although it could be contributing to the possibility of decreases in EBA months. Overall, the positive long-tailed PDF projections suggest a trend toward the summer season becoming a more important source for EBA months.

Although large uncertainties are associated with these projections, we would argue that the inclusion of structural uncertainty in both the candidate ecological models and the downscaled GCMs is still a more informative

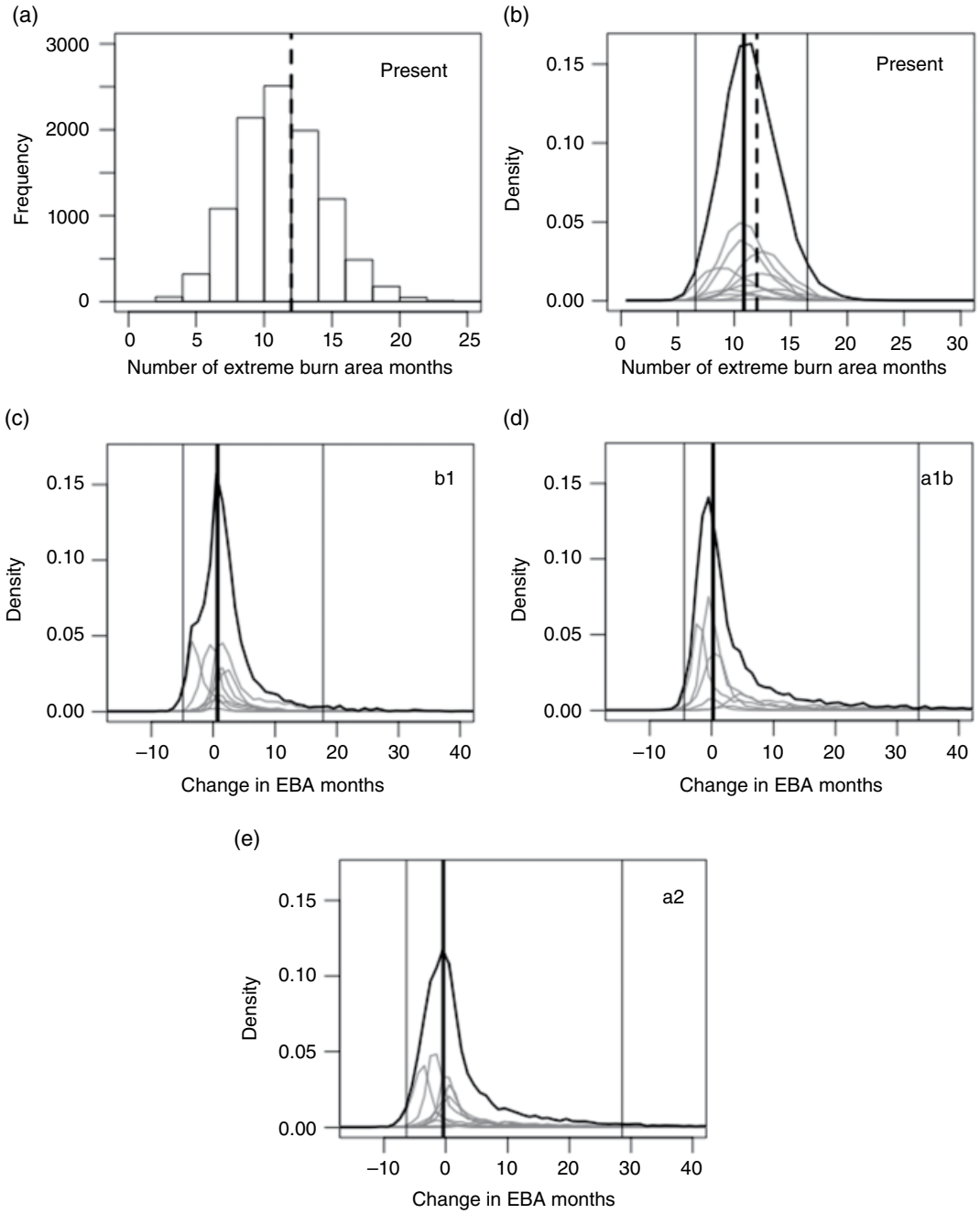

Figure 16.2 (a) Histogram of 10,000 simulations from the five-fold cross-validated ecological model and the verifying observation (vertical dashed line) of the number of EBA months (>4047 ha) for the period 1980–2009. (b) BMA PDF of the predicted number of EBA months for the period 1980–2009 for the joint ecological-climate model. Verifying observation is the dashed vertical line, fiftieth percentile is the solid thick vertical line, thin vertical lines cover the 95% interval, and grey lines are individual GCM PDFs. (c) BMA PDF of projected difference between the number of EBA months in 2070–2099 versus 1980–2009 for the b1 emission scenario. (d) Same as (c) but for the a1b emission scenario. (e) Same as (c) but for the a2 emission scenario.

and faithful depiction of our current knowledge about how ACC could impact EBA months. In contrast, simple point projections would likely result in a truncated uncertainty range that is underdispersive and overconfident [*Terando et al.*, 2012]. The long tails showing nonnegligible probabilities of increasing EBA months indicate that large damages in the future cannot be completely discounted from a risk assessment by a decision maker, even

though the entirety of the PDFs spans positive (more EBA months) and negative values (fewer EBA months). Somewhat analogous to the uncertain estimates of the Earth's climate sensitivity to a doubling of CO_2 [*Knutti and Hegerl*, 2008], decision-relevant predictions with PDFs that are characterized by asymmetric tails may warrant special scrutiny of the potential consequences of the more extreme, but still possible, future state of nature.

Predictions about climate change are characterized by deep uncertainty [*Lempert*, 2002]. This is an inherent characteristic of climate change models and represents a major challenge for decision analysts who are trying to appropriately estimate and incorporate uncertainty into decision frameworks, and for decision makers, who ultimately have to choose among alternative actions. We address one such consequence, namely, extreme wildfire months in the southeastern United States. Extreme events represent a unique class of possible outcomes in the advent of climate change. Uncertainty is compounded by the lack of observations that can be used to predict future occurrences, and this low probability of occurrence could lead to an undervaluation of importance in decision problems. Such events may have profound consequences on many human endeavors, including land management decisions, and thus, their inclusion and treatment in decision problems is warranted [*Lempert et al.*, 2002].

Much of the impetus for characterizing and quantifying the different sources of uncertainty is for use in decision making wherein we directly incorporate the different sources of uncertainty into predictive models evaluating the consequences of potential actions [*Walters*, 1986]. Ignoring this uncertainty in decision analysis results in overconfidence not only in the effects of our actions, but also in the robustness of our decisions. Therefore, we subscribe to and support the idea that providing probabilistic measures of events (e.g., EBA months) using all available information and uncertainties is an essential step in decision making.

Incorporating uncertainties derived from climate change models has not been handled explicitly in most land-management decision problems, although several authors have proposed a framework for doing so [cf., *Conroy et al.*, 2011; *Nichols et al.*, 2011], while recognizing two potential challenges. The first is the realization that land managers do not have control over actions (e.g., emission controls) that might affect the course of climate change dynamics, and the second is that quantifying and predicting changes in the climate system is not a trivial matter. We have attempted to address the latter by coupling an estimate of climatic change uncertainty with the *extradisciplinary* structural uncertainty present in ecological models to predict how climate change effects the system dynamics of interest (e.g., wildfire).

Several caveats and limitations apply to our approach used for quantifying uncertainty in global change prediction problems. First, our model projections assume that fuel characteristics remain stationary through time. If fuel loads or fuel types change, even moderately, the projections are less likely to hold. Second, suppression (both direct and indirect through urbanization) could change through time, which would have an attendant effect on the changing EBA probabilities.

As a final caveat, we stress that model weighting continues to be a subject of great debate within the climate impacts community [cf., *Knutti*, 2010]. Prior studies have shown that applying model weights to GCMs can result in overconfident projections [*Terando et al.*, 2012] while equally weighted projections did not. Such a risk would also apply in this study and future work could incorporate projections that also derive projections from equally weighted GCM ensembles. However, as noted in *Knutti* [2010], the line between unweighted and weighted model ensembles is not so clear cut considering that other, implicit forms of model weighting are commonly practiced. For instance, older generations of GCMs are continually cast aside in climate impact studies, which in effect places a weight of zero on these GCMs. In addition, some GCMs may share similar "DNA" [*Masson and Knutti*, 2011], which in effect results in higher weights being placed on models with shared or very similar parameterizations and subroutines.

Our view is that fully using the information contained within the observations in order to construct a model-weighted prediction still has merit if done judiciously and with careful consideration of the trade-offs. From a decision-making perspective, a high utility outcome might involve a weighted prediction that is frequently updated as new data (and new models) are received, thus allowing managers to estimate new expected values for the portfolio of actions available to them. Such situations currently exist in areas such as hurricane forecasts [*Hamill et al.*, 2011] and wildlife harvesting limits [*Nichols et al.*, 2007]. Bringing this type of system to the realm of global change problems is daunting but perhaps necessary for realizing successful climate adaptation strategies. This study continues toward this goal by providing examples of how model weighting could be undertaken in joint ecology-climate modeling problems.

In this chapter, we presented an explicit framework that couples multiple sources of uncertainty from different disciplines into probabilistic global change projections. This coupling could have significant implications for decision makers as it represents a quantitative end point that can be incorporated into a myriad of land management and hazard mitigation decision problems. Our intent was to underscore the potential value of this estimation problem in decision making and stimulate further discussion and research in this area.

Further advances in uncertainty estimation and model weighting will provide an opportunity to improve the quality of uncertainty estimates for optimization of actions or for the development of robust climate adaptation strategies.

ACKNOWLEDGMENTS

We thank the two anonymous reviewers and J. Littell for their comments and insights, which greatly improved this work. Any use of trade, product, or firms' names is for descriptive purposes only and does not imply endorsement by the US government.

REFERENCES

Beganyi, S. R., and D. P. Batzer (2011), Wildfire induced changes in aquatic invertebrate communities and mercury bioaccumulation in the Okefenokee Swamp, *Hydrobiologia*, *669*(1), 237–247; doi:10.1007/s10750-011-0694-4.

Bhoi, S., J. Qu, and S. Dasgupta (2009), Multi-sensor study of aerosols from 2007 Okefenokee forest fire, *J. Appl. Remote Sens.*, *3*(1), 031501; doi:10.1117/1.3078070.

Brier, G. W. (1950), Verification of forecasts expressed in terms of probability, *Monthly Weather Rev.*, *78*(1), 1–3.

Brocker, J., and L. a. Smith (2008), From ensemble forecasts to predictive distribution functions, *Tellus A*, *60*(4), 663–678; doi:10.1111/j.1600-0870.2008.00333.x.

Brown, J. K., and J. K. Smith (2000), *Wildland fire in ecosystems: Effects of fire on flora*, Gen. Tech., edited by J. K. Brown and J. K. Smith, USDA Forest Service, Rocky Mountain Research Station, Ogden, UT.

Certini, G. (2005), Effects of fire on properties of forest soils: A review, *Oecologia*, *143*(1), 1–10; doi:10.1007/s00442-004-1788-8.

Cole, S. (2001), *An Introduction to Statistical Modeling of Extreme Values*, Springer, London.

Conroy, M. J., M. C. Runge, J. D. Nichols, K. W. Stodola, and R. J. Cooper (2011), Conservation in the face of climate change: The roles of alternative models, monitoring, and adaptation in confronting and reducing uncertainty, *Biol. Conserv.*, *144*(4), 1204–1213; doi:10.1016/j.biocon.2010.10.019.

Costanza, J. K., A. J. Terando, A. J. McKerrow, and J. A. Collazo (2015), Modeling climate change, urbanization, and fire effects on *Pinus palustris* ecosystems of the southeastern U.S., *J. Environ. Man.*, *151*, 186–199; doi:10.1016/j.jenvman.2014.12.032.

Dennison, P. E., S. C. Brewer, J. D. Arnold, and M. A. Moritz (2014), Large wildfire trends in the western United States, 1984–2011, *Geophys. Res. Lett.*, *41*(8), 2928–2933; doi:10.1002/2014GL059576.

Draper, D. (1995), Assessment and propagation of model uncertainty, *J. R. Statist. Soc. B*, *57*(1), 45–97.

Draper, D. (2013), Bayesian model specification: Heuristics and examples, Oxford Scholarship, 702, in *Bayesian Theory and Applications*, edited by P. Damien, P. Dellaportas, N. G. Polson, and D. A. Stephens, Oxford University Press, Oxford.

Fishman, S., A. Erez, and G. A. Couvillon (1987), The temperature dependence of dormancy breaking in plants: Mathematical analysis of a two-step model involving a cooperative transition., *J. Theor. Biol.*, *124*(4), 473–483.

Fried, J. S., M. S. Torn, and E. Mills (2004), The impact of climate change on wildfire severity: A regional forecast for northern California, *Clim. Change*, *64*(1–2), 169–191; doi:10.1023/B:CLIM.0000024667.89579.ed.

Frost, C. C. (1993), Four centuries of changing landscape patterns in the longleaf pine ecosystem, edited by S. Hermann, *Proc. Tall Timbers Fire Ecol. Conf.*, *18*, 17–43.

Frost, C. C. (2006), History and future of the longleaf pine ecosystem, 9–48, in *Longleaf Pine Ecosystems: Ecology, Management, and Restoration.*, edited by S. Jose, E. Jokela, and D. Miller, Springer, New York.

Girardin, M. P., and M. Mudelsee (2008), Past and future changes in Canadian boreal wildfire activity, *Ecol. Appl.*, *18*(2), 391–406; doi:10.1890/07-0747.1.

Gneiting, T., F. Balabdaoui, and A. E. Raftery (2007), Probabilistic forecasts, calibration and sharpness, *J. R. Stat. Soc. B*, *69*(2), 243–268.

Guttman, N. B. (1998), Comparing the Palmer Drought Index and the Standardized Precipitation Index, *J. Amer. Water Resour. Assoc.*, *34*(1), 113–121.

Hamill, T. M., J. S. Whitaker, M. Fiorino, and S. G. Benjamin (2011), Global Ensemble predictions of 2009's tropical cyclones initialized with an Ensemble Kalman Filter, *Monthly Weather Rev.*, *139*(2), 668–688; doi:10.1175/2010MWR3456.1.

Hawkins, E., and R. Sutton (2009), The potential to narrow uncertainty in regional climate predictions, *Bull. Amer. Meteor. Soc.*, *90*(8), 1095–1107.

Knutti, R. (2010), The end of model democracy?, *Clim. Change*, *102*(3–4), 395–404; doi:10.1007/s10584-010-9800-2.

Knutti, R., and G. C. Hegerl (2008), The equilibrium sensitivity of the Earth's temperature to radiation changes, *Nat. Geosci.*, *1*(11), 735–743; doi:10.1038/ngeo337.

Lempert, R., S. Popper, and S. Bankes (2002), Confronting surprise, *Soc. Sci. Comput. Rev.*, *20*(4), 420–440; doi:10.1177/089443902237320.

Lempert, R. J. (2002), A new decision sciences for complex systems., *Proc. Nat. Acad. Sci., 99, Suppl 3*, 7309–13; doi:10.1073/pnas.082081699.

Litschert, S. E., T. C. Brown, and D. M. Theobald (2012), Historic and future extent of wildfires in the Southern Rockies ecoregion, USA, *For. Ecol. Man.*, *269*, 124–133; doi:10.1016/j.foreco.2011.12.024.

Littell, J. S., D. McKenzie, D. L. Peterson, and A. L. Westerling (2009), Climate and wildfire area burned in western U.S. ecoprovinces, 1916–2003, *Ecol. Appl.*, *19*(4), 1003–1021; doi:10.1890/07-1183.1.

Liu, Y., S. Goodrick, and W. Heilman (2014), Wildland fire emissions, carbon, and climate: Wildfire-climate interactions, *For. Ecol. Man.*, *317*(SI), 80–96; doi:10.1016/j.foreco.2013.02.020.

Lorenz, E. N. (1963), Deterministic nonperiodic flow, *J. Atmos. Sci.*, *20*(2), 130–141.

Masson, D., and R. Knutti (2011), Climate model genealogy, *Geophys. Res. Lett.*, *38*(8), n/a–n/a; doi:10.1029/2011GL046864.

Maurer, E. P., A. W. Wood, J. C. Adam, D. P. Lettenmaier, and B. Nijssen (2002), A long-term hydrologically based dataset of land surface fluxes and states for the conterminous United States, *J. Climate*, *15*(22), 3237–3251.

Meehl, G. a., C. Covey, K. E. Taylor, T. Delworth, R. J. Stouffer, M. Latif, B. McAvaney, and J. F. B. Mitchell (2007),

The WCRP CMIP3 multimodel dataset: A new era in climate change research, *Bull. Amer. Meteor. Soc.*, *88*(9), 1383–1394; doi:10.1175/BAMS-88-9-1383.

Nakicenovic, N., et al. (2000), *Special report on emissions scenarios: A special report of Working Group III of the Intergovernmental Panel on Climate Change*, edited by N. Nakicenovic and R. Swart, Cambridge University Press, Cambridge.

Nichols, J. D., M. C. Runge, F. A. Johnson, and B. K. Williams (2007), Adaptive harvest management of North American waterfowl populations: a brief history and future prospects, *J. Ornithol.*, *148*(S2), 343–349; doi:10.1007/s10336-007-0256-8.

Nichols, J. D., M. D. Koneff, P. J. Heglund, M. G. Knutson, M. E. Seamans, J. E. Lyons, J. M. Morton, M. T. Jones, G. S. Boomer, and B. K. Williams (2011), Climate change, uncertainty, and natural resource management, *J. Wild. Man.*, *75*(1), 6–18; doi:10.1002/2010-33.

Noss, R., E. LaRoe, and J. Scott (1995), Endangered ecosystems of the United States: a preliminary assessment of loss and degradation, *Biological Report 28*, US Department of the Interior National Biological Service, Washington, D.C.

Palmer, T. N., G. J. Shutts, R. Hagedorn, F. J. Doblas-Reyes, T. Jung, and M. Leutbecher (2005), Representing model uncertainty in weather and climate prediction, *Ann. Rev. Earth Planet. Sci.*, *33*(1), 163–193; doi:10.1146/annurev.earth.33.092203.122552.

Peet, R. K. (2006), Ecological classification of longleaf pine woodlands, 51–94, in *Longleaf Pine Ecosystems: Ecology, Management, and Restoration*., edited by S. Jose, E. Jokela, and D. Miller, Springer, New York.

Peet, R. K., and D. J. Allard (1993), Longleaf pine vegetation of the Southern Atlantic and Eastern Gulf Coast Regions: A preliminary classification, in *The Longleaf Pine ecosystem: Ecology, restoration and management*, edited by S. M. Hermann, *Proc. Tall Timbers Fire Ecol. Conf*. *18*, 45–81.

Poulter, B., N. L. Christensen, and P. N. Halpin (2006), Carbon emissions from a temperate peat fire and its relevance to interannual variability of trace atmospheric greenhouse gases, *J. Geophys. Res.*, *111*(D6), D06301; doi:10.1029/2005JD006455.

Raftery, A. E., D. Madigan, and J. A. Hoeting (1997), Bayesian model averaging for linear regression models, *J. Amer. Stat. Assoc.*, *92*(437), 179–191.

Raftery, A. E., T. Gneiting, F. Balabdaoui, and M. Polakowski (2005), Using Bayesian model averaging to calibrate forecast ensembles, *Monthly Weather Rev.*, *133*(5), 1155–1174; doi:10.1175/MWR2906.1.

Richardson, C. J. (2012), Pocosins evergreen shrub bogs of the Southeast, 189–202, in *Wetland Habitats of North America: Ecology and Conservation Concerns*, edited by D. P. Batzer and A. Baldwin, University of California Press, Berkeley, CA.

Ryan, K. C., E. E. Knapp, and J. M. Varner (2013), Prescribed fire in North American forests and woodlands: history, current practice, and challenges, *Front. Ecol. Environ.*, *11*(s1), e15–e24; doi:10.1890/120329.

Sriver, R. L., N. M. Urban, R. Olson, and K. Keller (2012), Toward a physically plausible upper bound of sea-level rise projections, *Clim. Change*, *115*(3–4), 893–902; doi:10.1007/s10584-012-0610-6.

Stoner, A. M. K., K. Hayhoe, X. Yang, and D. J. Wuebbles (2013), An asynchronous regional regression model for statistical downscaling of daily climate variables, *Int. J. Climatol.*, *33*(11), 2473–2494; doi:10.1002/joc.3603.

Terando, A., K. Keller, and W. E. Easterling (2012), Probabilistic projections of agro-climate indices in North America, *J. Geophys. Res.*, *117*(D8), D08115; doi:10.1029/2012JD017436.

US Fish and Wildlife Service (2007), OkefenokeeFire, *Big Turnaround Fire Biggest Most Expens. FWS*, available from http://www.fws.gov/fire/news/ga/big_turnaround_fire.shtml.

US Fish and Wildlife Service (2012), Honey Prairie Fire Declared Out (912), available from http://www.fws.gov/okefenokee/PDF/honey prairie fire declared out.pdf.

Walsh, J., et al. (2014), Our changing climate, 19–67, in *Climate Change Impacts in the United States: The Third National Climate Assessment*, edited by J. M. Melillo, T. C. Richmond, and G. W. Yohe, US Global Change Research Program.

Walters, C. (1986), *Adaptive Management of Renewable Resources*, Macmillan Pub. Co., New York.

Wintle, B. A., M. A. McCarthy, C. T. Volinsky, and R. P. Kavanagh (2003), The use of Bayesian model averaging to better represent uncertainty in ecological models, *Conserv. Biol.*, *17*(6), 1579–1590; doi:10.1111/j.1523-1739.2003.00614.x.